

Research on performance optimization of NOMA-VLC based on LWT

line 1: 1st ShenBo
line 2: Department of Process
Technology
line 3: Xi'an Institute of
Electromechanical Information
Technology
line 4: XiAn, China
line 5: liangshui2000@163.com

line 1: 2nd FanXin
line 2: School of Electronic
Information Engineering
line 3: Xi'an Technological
University
line 4: XiAn, China
line 5: 3465600100@qq.com

line 1: 3rd ZhangFeng
line 2: School of Electronic Information
Engineering
line 3: Xi'an Technological University
line 4: XiAn, China
line 5: zf_zx963@163.com

Abstract— NOMA-VLC system based on FFT-OFDM has low reliability and poor user fairness. Therefore, this paper proposes to establish a NOMA-VLC system based on LWT-OFDM by using Lifting Wavelet Transform (LWT) as a carrier modulation method. Firstly, the user channel characteristics of NOMA-VLC system are derived, and the causes of poor reliability and user fairness are analyzed; On this basis, the LWT-OFDM signal decomposition and reconstruction formula is derived; Finally, multi-user correct demodulation is achieved at the receiving end by serial interference detection technology. The experimental results of the indoor space of $4m \times 4m \times 3m$ show that: The transmission efficiency of the proposed system is improved compared with that of FFT-OFDM system; When the average BER is 10^{-4} the reliability of the proposed method is improved by at least 7dB and the user fairness is improved by at least 1.4dB compared with the NOMA-VLC system based on FFT-OFDM; The communication system using sym4 wavelet base has better reliability and fairness among users; With the improvement of front-end modulation order, the performance of this method in reliability and fairness is more significant. The proposed method provides a guarantee for indoor visible light communication in multi-user scenarios.

Keywords—NOMA technology; Lifting wavelet algorithm; User reliability; User Fairness

I. INTRODUCTION

At present, networking communication in multi-user scenarios is a research hotspot in Visible Light Communication (VLC) [1-2]. VLC systems are generally based on FFT to implement DC-biased Optical OFDM (DCO-OFDM) [3] systems, but their communication reliability cannot fully meet the requirements in multi-user scenarios.

Literature[4] proposes that non-orthogonal multiple access (NOMA) provides an effective means for networking applications and multi-user communication by increasing power domain multiplexing. Since it is unrealistic for all users to access the same time-frequency resource, a NOMA-VLC system based on FFT-OFDM is proposed. Literature [5-6] proposes that the traditional DCO-OFDM system is based on Fast Fourier Transform (FFT) modulation, and the convolution operation of FFT increases the complexity of the system. At the same time, the FFT-OFDM system reduces the interference between carriers by adding CP and protection intervals, but increases the system complexity and reduces the transmission efficiency. Literature [7-8] proposes an OFDM system based on DWT, which improves the performance of the FFT-OFDM system, but the wavelet basis function used in it increases the computational complexity of the system. Literature [9] proposes that LWT-OFDM be applied to VLC, by comparing the LWT-OFDM system with the FFT-OFDM system, the results show that the LWT-OFDM system has a good effect, but the system reliability is not considered.

Literature[10] proposes that LWT inherits the MAR characteristics, scale orthogonal characteristics, translational orthogonal characteristics, no more convolution, and the complexity of the relative FFT process is reduced. At the same time, the LWT is constantly rounded through the lifting process, converts floating-point operations to integer operations, improves conversion accuracy, and saves hardware implementation resources.

In order to further improve the performance of the VLC system and take into account the communication reliability and user fairness, this paper proposes to implement the NOMA-OFDM system based on LWT and apply it to the indoor VLC system, so that the reliability can be ensured in the multi-user scenario and the fairness difference between users can be reduced.

II. NOMA-VLC SYSTEM MODEL

A. VLC channel modeling in multi-user scenarios

In the VLC system, ideally the VLC system channel is in a linear time-invariant state. The light source radiation model of the indoor VLC system is in Fig 1:

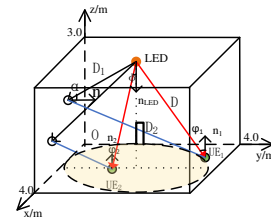


Fig. 1. Radiation Model of Geometric Scene for VLC System

Through the impulse response of the receiver, the channel characteristics of VLC can be expressed as^[4]:

$$h(t; R_s; R_r) = \sum_{k=0}^{\infty} h^{(k)}(t; R_s; R_r) \quad (1)$$

In equation (1), R_s is the characteristic of the receiver, including position and direction vectors; R_r represents the characteristics of the receiver, including the position vector, the area of the photodetector, the receiving angle.

At $g = 0$, the LED signal reaches the receiver through line-of-sight transmission; At $g = 1$, the LED signal reaches the receiver through the non-line-of-sight transmission channel. At $g = 0$, which is the ideal VLC channel, the impulse response can be expressed as:

$$h(t; R_s; R_r) = T(\phi) \frac{A_r \times \cos(\phi)}{D^2} \delta(t - \frac{D}{c}) \quad (2)$$

In Equation (2), Ar is the photodetector receiving area; φ is the angle of incidence of the photodetector; c is the speed of light; $D = |\vec{R}_s - \vec{R}_r|$. The LED light source Lambertian radiation pattern $T(\phi)$ can be expressed as:

$$T(\phi) = \frac{k+1}{2\pi} \cos^k(\phi) \quad (3)$$

In equation (3), k is the Lambertian index and ϕ is the emission angle. And the distance D between the sender and receiver of user 1 can be represented according to Figure 1:

$$D = \frac{3}{\cos \phi} = \frac{3}{\cos \phi_1} \quad (4)$$

At the same time, due to the limitation of the LED signal propagation space in the room, the optical path difference is very small, and the channel gain of the non-direct link is negligible^[11]. Therefore, the paper only considers the direct link channel gain, which is expressed as:

$$H_{DC}(0; R_s; R_r) = \int_{-\infty}^{\infty} h(t; R_s; R_r) dt = \frac{(k+1)Ar \cos(\phi)}{2\pi D^2} \cos^k(\phi) \quad (5)$$

The signal power of the receiver is:

$$P_s = P_r H_{DC}(0; R_s; R_r) \quad (6)$$

In equation (6), P_s, P_r represents the power at the sender and the receiver. Further derivation yields the channel can be expressed as:

$$H_E = P_s / P_r \quad (7)$$

Finally, the indoor VLC channel is modeled and the channel gain model is obtained as shown in Figure 2:

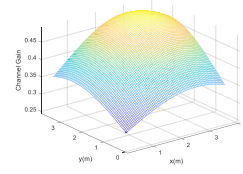


Fig. 2 Channel Gain Model of Indoor VLC System

In the 3D stereogram shown in Figure 2, the X axis represents the abscissa of the position, the Y axis represents the ordinate of the position, and the Z axis represents the channel gain. The channel gain value of edge users who can be far away from the LED is smaller than that of intermediate users who are closer to the LED. Therefore, the channel gain is large when the channel environment is good, and the channel gain is small when the channel environment is poor, which indicates that there is a large difference in channel gain between users of VLC system, which will lead to poor communication reliability and obvious performance differences between users.

B. NOMA-VLC system model

In order to realize the preliminary optimization of DCO-OFDM-VLC, NOMA technology is introduced to realize the NOMA-VLC system based on FFT-OFDM. The block diagram of the VLC system of NOMA-OFDM is shown in Fig 3:

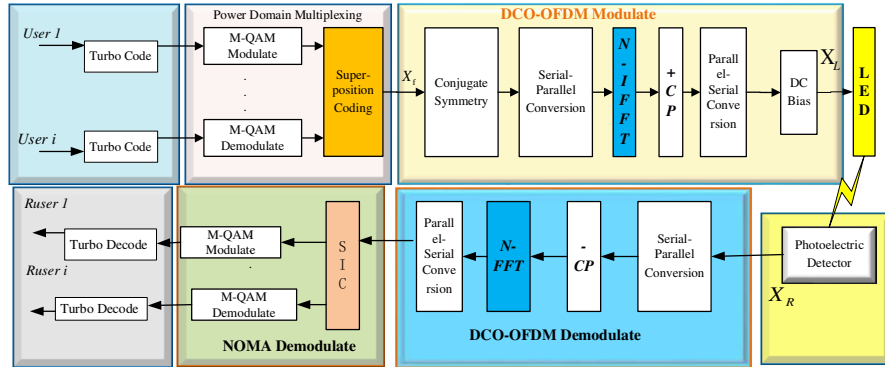


Fig. 3 NOMA-OFDM-VLC system block diagram

From Fig 3, at the sender, N user signals are used Turbo coding, and then through QAM modulation. Combined with the VLC channel model simulation result map, it can be obtained that there are channel differences between users, and the power distribution is carried out according to the FPA. Using superposition coding technology, integrating multi-user information, that is, completing the NOMA modulation. Then by conjugate symmetry, by series parallel conversion, OFDM modulation, and finally pass VLC channel transmission; At the receiver, PD collects signals and demodulates them through OFDM, and realizes multi-user separation through SIC technology.

And in Figure 3, the sender will allocate the power to be transmitted according to certain rules X_f is represented as:

$$X_f = \hat{X}_1 = [X_0, X_1, \dots, X_{i-1}] \quad (8)$$

In equation (8), $X_{i-1} = \sum_{j=1}^M \sqrt{p_{i,j}} x_{ij}$, stands for NOMA Power

Domain Multiplexing., $p_{i,j}$ represents the power of the user in the specified subcarrier. The expression for the FPA method chosen in the paper is expressed as:

$$P_i = \alpha_{fpa} P_m \quad (9)$$

In equation (9), P_i is the power of user i , and α_{fpa} represents the power distribution factor, moreover, $0 \leq \alpha_{fpa} \leq 1$. Therefore, the channel conditions are poor, and the allocated power is large. When the α_{fpa} is determined, the power allocated by the user is determined, so the process of designing the receiver is simple, it is necessary to solve the problem of poor reliability caused by serious user interference. The specific values of α_{fpa} can be expressed as:

$$\alpha_{jpa} = H_i / \sum_{i=1}^I H_i \quad (10)$$

To ensure that the signal is transmitted to real numbers, the OFDM symbol is Emit symmetry. At the same time guaranteed $X_0 = X_{I/2} = 0$, as follows:

$$X_N = \hat{X}_{iDCO-FFT} = [0, X_1, \dots, X_{\frac{I}{2}-1}, 0, X_{\frac{I}{2}-1}^*, \dots, X_1^*] \quad (11)$$

Equation (11) represents the results of input signal when the DCO-OFDM uses FFT. Do N-point IFFT on X_N and add the cyclic prefix CP, etc. The signal can be expressed as X_L ,

$$X_L = \frac{1}{\sqrt{N}} \sum_{k=0}^{N-1} X_N \exp\left(\frac{j2\pi kn}{N}\right) + X_{\text{IFFT-CP}}, \quad n=1, 2, \dots, N \quad (12)$$

At the receiver, the received signal is demodulated by SIC, the basic principle is: Sort the channel gain from large to small, then demodulate it in descending order, cycle the operation until all multiple access interference is eliminated. The expression for the received signal X_R can be expressed as:

$$X_R = h_{i,j} X_L + n_i \quad (13)$$

In Equation (13), $h_{i,j}$ represents the channel gain of the user, n_i represents the noise information of the i-th user.

III. LWT-BASED NOMA-VLC SYSTEM

A. The principle of Lifting Wavelet Transform

The FFT-OFDM system has high computational complexity due to the convolution operation of FFT, unsatisfactory orthogonality causes poor reliability^[5]. So the LWT algorithm is introduced in this paper. LWT have the following advantages^[9-10]: the wavelet transform coefficients are integers, easy to reconstruct, and can be operated in situ. Compared with the FFT-OFDM system, LWT does not need to be convoluted and add CP, so the structure is simple and the computational complexity is low. The LWT forward and reverse transformations are shown in Figures 5 and 6:

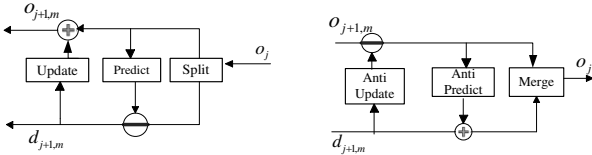


Fig5(a)LWT positive transformation (b) LWT inverse transformation

From Fig 5(a),(b): the LWT positive transform is divided into splitting, prediction, update, the LWT inverse transformation is divided into anti-update, counter-prediction and merger. LWT performs positive and inverse transformations on the initial signal through the prediction operator and update operator in the wavelet boosting algorithm. And the positive transformation process of LWT is as follows:

(1)Splitting: Divide the signal X_i into an even sequence o_{i+1} and an odd sequence d_{i+1} :

$$o_{i+1} = X_{i,2n}; d_{i+1} = X_{i,2n+1} \quad (14)$$

(2)Prediction: Select the strategy P and predict d_{i+1} with o_{i+1} :

$$d_{i+1,m} = d_{i+1} - P(o_{i+1}) \quad (15)$$

In Equation (15), $d_{i+1,m}$ is the prediction error, which is the high-frequency wavelet coefficient.

(3) Update: Select the policy U and update $d_{i+1,m}$ with U :

$$o_{i+1,m} = o_{i+1} + U(d_{i+1,m}) \quad (16)$$

In Equation (16), $o_{i+1,m}$ is called the scale coefficient, that is, the low-frequency wavelet coefficient. The selection of policy P and policy U is as follows:

$$P(o_{i+1,k}) = (o_{i+1,k} + o_{i+1,k+1}) / 2 \quad k \in \mathbb{N} \quad (17)$$

$$U(d_{i+1,k}) = (d_{i+1,k} + d_{i+1,k+1}) / 4 \quad k \in \mathbb{N}$$

B. LWT-based OFDM system

The LWT inherits the MRA characteristics of the first generation of wavelet transform, which meets the requirements of the OFDM system for frequency band and carrier orthogonality, and improves communication reliability. Therefore, an OFDM system based on LWT is proposed, which uses the wavelet function as a subcarrier, obtains the LWT-OFDM modulated signal after ILWT, and then reaches the receiver through channel transmission, and the receiver uses LWT demodulation^[9]. The system block diagram is shown in Fig 6:

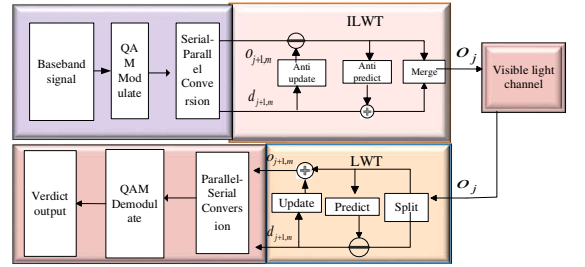


Fig.6 OFDM system block diagram based on LWT

From Fig.6, at the sender, through QAM modulation, series and conversion to obtain N signals, ILWT modulation, the N signal is converted into a signal, and LWT-OFDM signals are generated, which are transmitted through the visible light channel. At the receiver, demodulated by LWT, the single signal collected at the receiver is converted into an N signal, and then the N signal is converted into a single signal by parallel series conversion, and the final judgment output is demodulated by QAM.

Among them, ILWT is the system modulation mode. The modulation block diagram is shown in Figure 7(a). LWT is the system demodulation method, and the demodulation block diagram is shown in Figure 7(b).

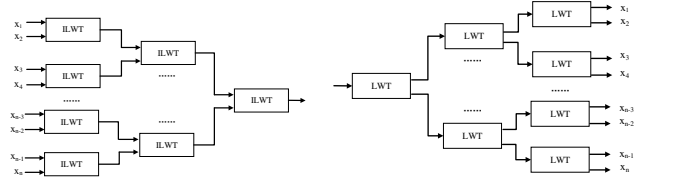


Fig. 7(a) Modulation schematic (b) Demodulation schematic

At the modulation end, the signal is represented as d_i^{i-1} and o_i^{i-1} , which are modulated by the LWT algorithm as equation (18):

$$\begin{cases} d_l^{i-1} = d_l^i + \sum_k p_k^i o_{l-k}^i \\ o_l^{i-1} = o_l^i + \sum_k u_k^i d_{l-k}^i \end{cases} \quad l = 0, 1, \dots, N/2 - 1 \quad (18)$$

In Equation (18), p is the prediction coefficient and u is the renewal coefficient.

At the demodulation end, after demodulation by the boosting algorithm, it is equation (19):

$$\begin{cases} o_l^i = o_l^{i-1} - \sum_k u_k^i d_{l-k}^{i-1} \\ d_l^i = d_l^{i-1} - \sum_k p_k^i o_{l-k}^i \end{cases} \quad l=0,1,\dots,N/2-1 \quad (19)$$

C. NOMA-VLC system based on LWT-OFDM

In order to realize the optimization of the performance of the NOMA-VLC system of FFT-OFDM, LWT-OFDM is proposed to replace FFT-OFDM combined with NOMA-VLC system. Replacing the FFT in the block diagram of the NOMA-VLC system in Figure 3 with the LWT is the core of the LWT-OFDM-based NOMA-VLC system, and then the high and low frequency signals generated by the enhanced wavelet transform are transmitted.

Firstly, on the sender, the LWT does not perform Emit symmetry, so update Equation (11) to get X_j as follows:

$$X_j = \hat{X}_{i_{DCO-LWT}} = [0, X_0, X_1, \dots, X_{\frac{i}{2}-1}, \dots, X_{i-1}] \quad (20)$$

Equation (20) represents the input signal processing result of DCO-OFDM using LWT modulation.

Secondly, combined with the LWT positive transformation formula, X_j is treated as X_i and X_j is processed.

Finally, according to the principle of NOMA and LWT, the NOMA-VLC system based on LWT-OFDM is established, and the wavelet symbol transmitted on the channel is a combination of high frequency coefficient and low frequency coefficient. Combined with the literature [8] derivation, the output signal of DCO-OFDM using LWT modulation can be expressed as:

$$X(i)_{LWT} = \frac{1}{\sqrt{N}} \left(\sum_i \tilde{x} o_{j+1,m} 2^{j/2} \phi[2^j m - i] + \sum_i \tilde{x} d_{j+1,m} 2^{j/2} \psi[2^j m - j] \right) \quad (21)$$

In Equation (21), j is the resolution, i is the scale, and \tilde{x} is the signal after constellation mapping and power

distribution. The final signal to be transmitted after ILWT modulation is $\hat{X}(i)_{LWT}$.

The signal $\hat{X}(i)_{LWT}$ to be transmitted passes through the visible light channel, and the received signal X_R of the LWT-OFDM-OFDM-based NOMA-VLC system can be obtained:

$$X_R = \sum_{i=1}^i \sqrt{p_i} H_i \hat{X}(i)_{LWT} + n_i \quad (22)$$

The receiving end performs reverse demodulation, that is, through LWT-OFDM demodulation, SIC demodulation and constellation demodulation, and finally achieve the correct demodulation of multiple users.

In visible light communication, the paper system and rate [4] are as follows:

$$R_i(m) = \frac{W_i}{2} \log_2 \left[1 + \frac{\gamma^2 \rho^2 H_i p_i}{\gamma^2 \rho^2 H_i \sum_{i=1}^i p_i + \gamma^2 H_i \sigma_{clip}^2 + 1} \right] \quad (23)$$

In Equation (23), γ is the photoelectric conversion factor, let $\gamma=1$; ρ be the attenuation factor, and σ_{clip} is the standard deviation of limiting noise. W_i represents the bandwidth of user i , if the total power of the system does not change, the system and rate only change with the system power allocation algorithm. The sum rate of the OFDM-VLC system is as follows:

$$R_i(m) = \frac{W_i}{2*U} \log_2 \left[1 + \frac{\gamma^2 \rho^2 H_i p_i}{\gamma^2 \rho^2 H_i \sum_{i=1}^i p_i + \gamma^2 H_i \sigma_{clip}^2 + 1} \right] \quad (24)$$

In Equation (24), U represents the number of users, and it can be seen that the OFDM-VLC system and rate vary with the number of users.

IV. EXPERIMENTS AND PERFORMANCE ANALYSIS

A. System experiment and parameter setting

Based on indoor VLC modeling, the three-dimensional spatial environment of $4m \times 4m \times 3m$ is constructed, user 1 is set at the center of the indoor space, user 2 is set at the edge, and the signals of user 1 and user 2 are detected by photodetectors. The experimental system is shown in Fig 8:

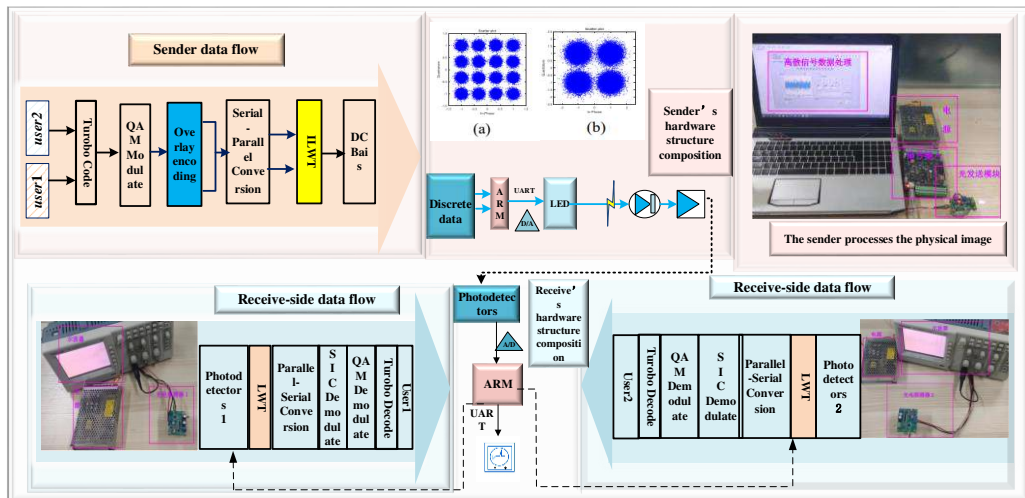


Fig. 8 Experimental system (a) User 1 pre-demodulation constellation diagram; (b) User 2 pre-demodulation constellation diagram

From Fig 8 ,experimental system is divided into one sender and two receivers. The sender sends the processed

signal $\hat{X}(i)_{LWT}$ through the arbitrary waveform signal generator, converts it through D/A, and then sends it through the optical

channel, then enhances by an amplifier (AMP-OPA657). The receiver probes the signal via a PIN, then processes it through A/D conversion and an ARM processor, and finally saves the waveform of the signal via an oscilloscope (Tektronix7354C). Finally, LWT-OFDM and SIC demodulation were carried out. The experimental parameters are shown in Tab 1. Parameter settings can be found in References [4], [9], [12], and [13].

In Figure 8, (a) and (b) are the constellation diagram of the received signal, respectively, the corresponding constellation diagram before user 1 and 2 demodulation. After user 1 is demodulated, user 2 is only affected by noise, so user 2 demodulation effect is better, so user 1 can be distinguished from user 2.

TABLE I. EXPERIMENTAL PARAMETERS

parameter	data
Room size	4m × 4m × 3m
LED luminous power/W	1
LED lighting intensity/cd	60
LED modulation bandwidth/HZ	5 × 10 ⁷
Subcarrier bandwidth/HZ	1.56 × 10 ⁶
Photoelectric conversion factor	1
LED FOV/°	70
Detector surface area/cm ²	1
Wall reflective area/cm ²	0.25
The reflectivity of the wall ρ_i	0.8
Platform communication distance(cm)	20
Turbo decoding method	Iterative decoding
OFDM modulation/demodulation mode	ILWT/LWT

At the same time, combining(23)and (24), the relationship between the number of users and communication and rate of the indoor VLC system simulated is shown in Figure 9:

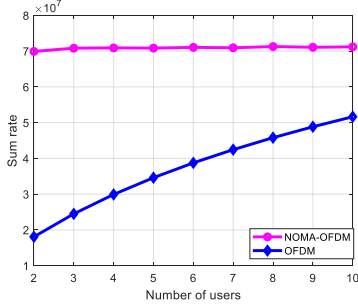


Fig.9 System and rate comparison curves

From figure 9, the communication rate of the NOMA-OFDM system is significantly higher than that of the OFDM system. At the same time, compared with the OFDM system, the sum rate of the NOMA-OFDM system is relatively stable, although it also shows a downward trend with the increase of the number of users in the system, but it is not significant

B. Transmission efficiency analysis

Combined (11) and (20), the total number of subcarriers is i , using M-QAM modulation mode, the amount of information carried by the DCO-FFT-OFDM system is $\log_M \frac{i}{2}$; the amount of information carried by the DCO-LWT-OFDM system is $\log_M i$; So the transmission efficiency of the DCO-LWT-OFDM system is increased by 50% compared to the DCO-FFT-OFDM System.

C. Analysis of communication reliability and user fairness

The number of users is selected as 2, and the modulation method is 4QAM. First, implement a NOMA-VLC system based on FFT-OFDM. Then implement a NOMA-VLC system based on LWT-OFDM., selects different wavelet bases at the same time .The average BER performance curve of the implemented method is compared, and the experimental results are shown in Fig 10(a). Select different wavelet basis functions ,and the implemented method will be analyzed for fairness performance, the experimental results are shown in Fig 10(b):

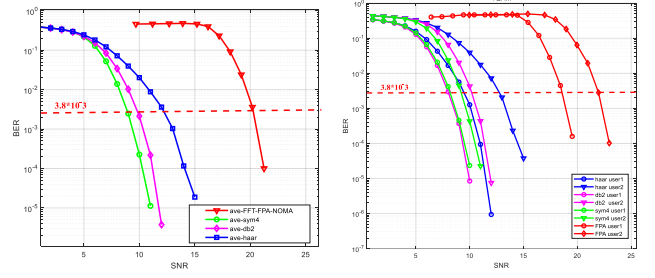


Fig. 10(a)Average BER Performance Curve of Different Wavelet Bases (b)Performance of 4QAM order

From Fig 10(a), the performance of the proposed system is better than the NOMA-VLC based on FFT-OFDM, and the choice of different wavelet bases will affect the reliability of system communication. When the average BER is 10^{-4} , the wavelet base performance of haar/db2/sym4 is improved by at least 7/9.3/10.9dB. When the RS threshold is reached, the haar/db2/sym4 wavelets have at least 7/9.5/10.5dB performance improvements. From Fig 10(b), when the BER is 10^{-4} , the difference in performance between user 1,2 of the NOMA-VLC based on FFT-OFDM is 4.5dB. The paper system selects haar/db2/sym4 wavelets, the performance difference between user 1,2 is 3.1/2.1dB. From the perspective of fairness, the fairness of the proposed system is better than that of the NOMA-VLC based on FFT-OFDM. It shows that the system in this article can provide a guarantee for user fairness. At the same time, the fairness performance of sym4 wavelets is better than that of haar wavelets and db2 wavelets.

D. Modulation order performance analysis

Different wavelet basis functions are selected and the implemented methods are compared and analyzed under different modulation orders, as shown in Fig10(b) and Fig11(a), (b):

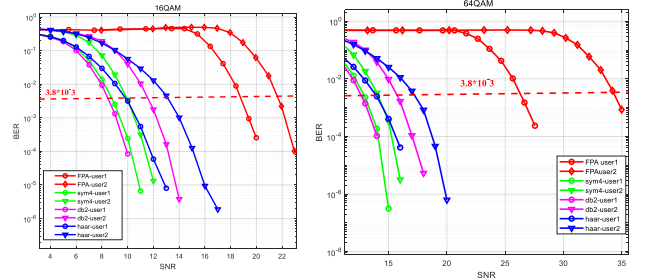


Fig. 11(a) Performance of 16QAM order (b) Performance of 64QAM order

The signal-to-noise ratio values required for users 1 and 2 to reach the RS threshold at different orders can be obtained from Fig10(b), Fig11(a), (b), as shown in Table 2:

TABLE II. PERFORMANCE OF DIFFERENT ORDER ALGORITHMS

Modulation order	User 1 RS threshold required SNR/(dB)				User 2 RS threshold required SNR/(dB)				User performance differences/(dB)			
	FFT-NOMA	haar	db2	sym4	FFT-NOMA	haar	db2	sym4	FFT-NOMA	haar	db2	sym4
4QAM	18.2	9.8	8.5	8.6	21.8	13.1	10.7	9.6	3.6	3.3	2.2	1.
16QAM	18.4	10.0	8.9	9.0	22	13.2	11.5	10.1	3.6	3.2	2.6	1.1
64QAM	26.7	14.2	13.1	13.2	34.1	17.3	15.7	14.2	7.4	3.1	2.6	1.

From Tab.2, the front-end modulation order has increased from 4 to 64, in terms of communication reliability, the NOMA-VLC system based on FFT-OFDM has 8.5dB performance degradation for user 1 and 12.3dB performance degradation for user 2. In this paper system, when the haar wavelet is selected, the performance of user 1 and user 2 decreases by about 4.6dB; When db2 wavelet is selected, the performance of user 1 and user 2 decreased by at least 4.6dB; When the sym4 wavelet is selected, the performance of user 1 and user 2 decreases by about 4.6dB.

The front-end modulation order is increased from 4 to 64, in terms of user fairness, the user fairness of the NOMA-VLC system based on FFT-OFDM is reduced by about 3.8dB. The paper system uses three different wavelet bases, and the user fairness performance does not degrade significantly with the modulation order increases.

In summary, when the front-end modulation order is high, the system in this paper is more conducive to ensuring the reliability of the communication system and the fairness between users, thus providing a good guarantee for high-order modulation and high-speed communication.

V. CONCLUSION

In order to ensure user fairness and improve communication reliability, a NOMA-VLC system based on LWT-OFDM is proposed to optimize the performance of VLC system. And conduct experimental tests and performance verification. Theoretical analysis and experimental results show that:

(1) The paper method effectively improves the communication reliability of OFDM-VLC system. When the average BER is 10^{-4} , Compared with the NOMA-VLC system of FFT-OFDM, the performance of the paper system under the haar/db2/sym4 wavelet base is improved by 7/9.3/10.9dB.

(2) The paper method effectively improves the user fairness of OFDM-VLC system. When the BER is 10^{-4} , the performance of the proposed system is improved by 1.4/2.5/3.5dB respectively compared with the NOMA-VLC system of FFT-OFDM under the haar/db2/sym4 wavelet base.

(3) With the improvement of the front-end modulation order, the fairness and reliability performance of the paper system users are better than that of the NOMA-VLC system of FFT-OFDM, which provides a good guarantee for the improvement of communication speed.

REFERENCES

- [1] M A Arfaoui, A Ghayeb, C Assi, et al. "CoMP-Assisted NOMA and Cooperative NOMA in Indoor VLC Cellular Systems [J]." in IEEE Transactions on Communications, pp. 6020-6034, Sept. 2022.
- [2] Zhang L, Fang F, Wu Z. "Energy Efficient Power allocation for OFDM-NOMA Visible Light Communication Systems With Statistical Channel State Information[J]." 2021 15th International Symposium on Medical Information and Communication Technology (ISMIC).
- [3] Assaidah A, Liu Y, Chow C W, et al. "Demonstration of Non-Hermitian Symmetry (NHS) IFFT/FFT Size Efficient OFDM Non-Orthogonal Multiple Access (NOMA) for Visible Light Communication [J]." IEEE Photonics journal, 2020(3):12.
- [4] ZHANG Feng, LIANG Yuanbo, ZHAO Li, LIANG Yuan. Performance optimization method of indoor visible light communication system based on non-orthogonal multiple access[J]. Infrared and Laser Engineering, 2021, 50(11):311-317.
- [5] Levent V E, Uysal M, Saglam G, et al. "FPGA Based DCO-OFDM PHY Transceiver for VLC Systems [J]." 2019 11th International Conference on Electrical and Electronics Engineering (ELECO). IEEE.
- [6] G Aykırı, B Avcı, A Özen. "M-CSK and M-QAM Modulated DCO-OFDM for Visible Light Communication Systems [J]." 2022 30th Signal Processing and Communications Applications Conference (SIU), 2022, pp. 1-4.
- [7] Pang J, Ni S, Wang F, et al. "Performance Analysis of FSO System Using FFT-OFDM and DWT-OFDM [J]." 2019 24th. International Conference on Photonics in Switching and Computing (PSC).
- [8] Khan A, Khan S, Baig S, et al. "Wavelet OFDM with overlap FDE for non-Gaussian channels in precoded NOMA based systems." [J]. Future Generation Computer Systems, 2019, 97:165-179.
- [9] Zhao Li, Dong Hang Hang, Zhang Feng. Visible DCO-OFDM System Based on LWT [J]. Acta Photonica Sinica, 2021, 50(5): 0506002
- [10] Gao Jian-bo, Zhao Er-yuan. A New OFDM System Based Lifting Wavelet Transform for Wireless Channel[J]. The Journal of China Universities of Posts and Telecommunications. 2005, 12(3):21-25.
- [11] JIA Kejun, HAO Li, YU Caihong. Multipath channel modeling and performance analysis of MIMO-ACO-OFDM system for indoor visible light communication[J]. Acta Optica Sinica, 2016, 36(07):57-68.
- [12] Ragnini D F, Vieira L C, Pohl A A P, et al. Constant response window channel estimation method and LUT-based digital predistortion applied to OFDM VLC links[J]. Optics Communications, 2020, 475: 126198.
- [13] Ngene C E, Thakur P, Singh G. "Analysis of Power Allocation in Visible Light-NOMA Communication Using Uniform Probability Distribution Function [J]." 2021 International Conference on Artificial Intelligence, Big Data, Computing and Data Communication Systems (ICABC)